



ELSEVIER

Journal of Non-Crystalline Solids 266–269 (2000) 1274–1278

JOURNAL OF
NON-CRYSTALLINE SOLIDS

www.elsevier.com/locate/jnoncrystal

p Channel thin film transistor and complementary metal–oxide–silicon inverter made of microcrystalline silicon directly deposited at 320°C

Y. Chen ^{*}, K. Pangal, J.C. Sturm, S. Wagner

Department of Electrical Engineering, Princeton University, Princeton, NJ 08544, USA

Abstract

We report a p channel thin film transistor (TFT) made of directly deposited microcrystalline silicon ($\mu\text{-Si}$). The $\mu\text{-Si}$ channel material is grown by plasma-enhanced chemical vapor deposition (PECVD) using dc excitation of a mixture of SiH_4 , SiF_4 and H_2 , in a process similar to the deposition of hydrogenated amorphous silicon (a-Si:H). The deposition temperature for the $\mu\text{-Si}$ is 320°C and the highest post-deposition TFT process temperature is 280°C. By integrating this p TFT on a single $\mu\text{-Si}$ film with an n channel TFT, we fabricated a complementary metal–oxide–silicon (CMOS) inverter of deposited $\mu\text{-Si}$. The p channel $\mu\text{-Si}$ TFT represents a breakthrough in low-temperature Si TFT technology because p channel TFTs of a-Si:H have not been available to date. The integrated CMOS inverter is the building block of a new digital circuit technology based on directly deposited $\mu\text{-Si}$. © 2000 Elsevier Science B.V. All rights reserved.

1. Introduction

Considerable interest [1,2] exists in developing a large-area silicon technology produced at temperatures <350°C. This technology should be capable of furnishing the standard devices, including transistors, rectifying diodes and photodiodes, for applications in macroelectronics [1], and for add-on electronics to application specific integrated circuits (ASICs) [2]. ASIC applications require that all process temperatures be <400°C. In general, a reduction of the process temperature expands the applicability of macroelectronics. A usable ultra low-temperature (<350°C) technology

needs p and n channels field-effect transistors, which are the building blocks for complementary digital circuits. Polycrystalline Si (poly-Si) TFTs are used for thin film complementary metal–oxide–silicon (CMOS) circuitry. However, the crystallization temperatures of 600°C employed for making polycrystalline silicon films motivate the search for a lower-temperature CMOS-capable Si TFT technology. n channel thin film transistors (TFTs) of hydrogenated amorphous silicon (a-Si:H), which can be made at temperatures of $\sim 250^\circ\text{C}$, are widely used in large-area electronics [3]. However, no p channel TFTs have been made of a-Si:H because of the density of states in the lower half of its gap. Here we report the fabrication of a p channel TFT with a channel of directly deposited $\mu\text{-Si}$. The resulting capability for CMOS circuits becomes a motive for developing TFTs with microcrystalline silicon ($\mu\text{-Si}$) channels. Because

^{*} Corresponding author. Tel.: +1-609 258 5902; fax: +1-609 258 1840.

E-mail address: yuc@ee.princeton.edu (Y. Chen).

direct deposition can be conducted at the relatively low temperature of plasma-enhanced chemical vapor deposition (PECVD) for a-Si:H [4,5], the low temperature of typically 300°C for direct deposition makes $\mu\text{-Si}$ accessible to a wider variety of substrates than those compatible with furnace and rapid thermal annealing [6]. Microcrystalline silicon also retains the advantages of a-Si:H such as film uniformity over large deposition areas.

n Channel TFTs made of directly deposited $\mu\text{-Si}$ have been reported earlier [7–11]. While $\mu\text{-Si}$ films can be obtained at temperatures as low as $\sim 200^\circ\text{C}$ [12], raising the growth temperature improves transistor performance, so that the $\mu\text{-Si}$ layers for these n channel TFTs typically were grown at higher temperatures, e.g., 350°C [8]. We fabricated the p channel thin film transistor from $\mu\text{-Si}$ deposited at 320°C , and processed the TFT at a maximum temperature of 280°C . We then integrated this p channel TFT with an n channel TFT to make the first $\mu\text{-Si}$ CMOS inverter. The $\mu\text{-Si}$ p channel TFT and integrated CMOS inverter are two key advances toward a complete, ultra low-temperature semiconductor technology based on directly deposited $\mu\text{-Si}$.

2. Experiments

We describe the $\mu\text{-Si}$ CMOS process with Fig. 1. Substrates were unpassivated Corning 7059 glass. Both the p type and the n type TFTs use one single directly deposited $\mu\text{-Si}$ layer as the conducting channel. The $\mu\text{-Si}$ channel material is grown by PECVD in a process similar to the deposition of a-Si:H, using dc excitation of a mixture of SiH_4 , SiF_4 and H_2 . The undoped channel and the p^+ and n^+ contact layers were grown by

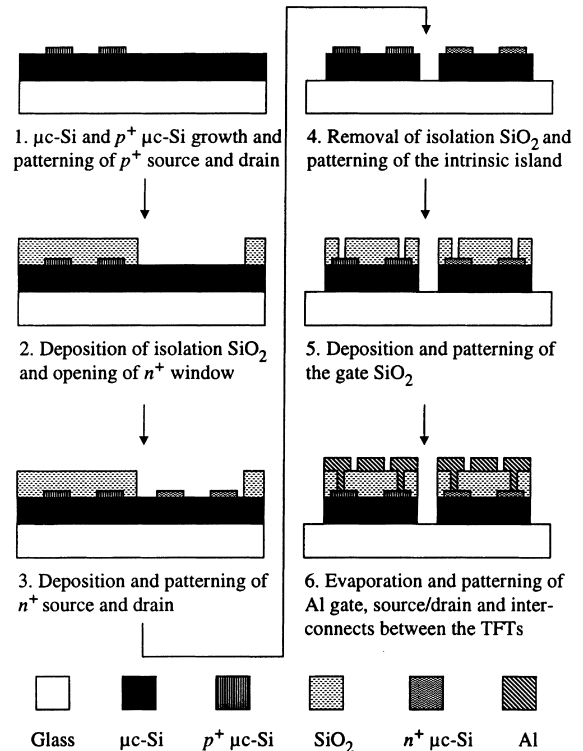


Fig. 1. Schematic process sequence for the $\mu\text{-Si}$ CMOS inverter.

PECVD in two separate (i layer, and doping) chambers. The SiO_2 gate dielectric also was grown by PECVD but in a separate system. Growth parameters are listed in Table 1. X-ray diffraction and Raman scattering [13], and an electron mobility of $4.9 \text{ cm}^2/\text{V s}$ in separately made n channel TFTs [10] prove that the films are microcrystalline. Adding SiF_4 to the source gas changes the growth chemistry [14], provides a wider range of structures [15], and a lower growth temperature [16] than

Table 1

Gas flow rates, deposition temperature, power density, pressure, and thickness of the films grown for the undoped $\mu\text{-Si}$ of the TFT channels, the doped source/drain contact layers, and the SiO_2 used for isolation

Layers	SiH_4 (sccm)	H_2 (sccm)	SiF_4 (sccm)	PH_3 , B_2H_6 , or N_2O (sccm)	Temperature ($^\circ\text{C}$)	Power density (mW/cm^2)	Pressure (mTorr)	Film thickness (nm)
$\mu\text{-Si}$	1	200	20	0	320	160	900	300
$\text{p}^+ \mu\text{-Si}$	2	100	0	50	280	324	900	60
$\text{n}^+ \mu\text{-Si}$	2	100	0	12	280	324	900	60
SiO_2	35	0	0	160	250	85	400	200

deposition from H_2 -diluted SiH_4 alone [15]. n channel TFTs of $\mu\text{-Si}$ grown with SiF_4 have the largest electron mobility reported to date [7]. The growth rate was 0.6 nm/s at a power density of 160 mW/cm². The dark conductivity of the i $\mu\text{-Si}$ is 1×10^{-7} S/cm, and its thermal activation energy is 0.55 ± 0.05 eV. The p^+ and n^+ source/drain contact layers were grown from SiH_4 , H_2 and B_2H_6 or PH_3 by RF excitation at 13.56 MHz. Their dark conductivities are 0.010 ± 0.001 S/cm (p^+ $\mu\text{-Si}$) and 20 ± 2 S/cm (n^+ $\mu\text{-Si}$).

The TFTs were made in the top-gate configuration shown in Fig. 1. The CMOS inverter is made of a p channel TFT and an n channel TFT of identical structure. A six-level mask process with masks designed in our laboratory were used in the inverter fabrication. The substrates were cleaned with the MICRO series 8790 glass-cleaning fluid (International Products Corporation) before deposition. First, 300 nm of i $\mu\text{-Si}$ and 60 nm of p^+ $\mu\text{-Si}$ layer were grown on the substrate without breaking vacuum. Next, we patterned the p^+ $\mu\text{-Si}$ source and drain for the p channel TFT using reactive ion etching (RIE) with 10% O_2 and 90% CCl_2F_2 . The deposition of a layer of 200 nm isolation SiO_2 followed. Then we opened a window in the SiO_2 using buffered oxide etch (BOE) to deposit a 60 nm n^+ $\mu\text{-Si}$ layer. After RIE patterning of the n^+ $\mu\text{-Si}$ source and drain for the n channel TFT, we removed the SiO_2 layer with BOE, and followed by the definition of the i $\mu\text{-Si}$ island using RIE. The channel $\mu\text{-Si}$ now exposed was exposed for 10 min to 1:3 $H_2O_2:H_2SO_4$ for oxidation, then dipped for 10 s in BOE, rinsed in de-ionized water, blow-dried in nitrogen, and immediately introduced in the system for gate insulator deposition. After we deposited 200 nm SiO_2 as gate insulator, we patterned the SiO_2 gate and opened contact holes to the n and p channels TFT source and drain using BOE. Then we thermally evaporated Al, and patterned the Al using a wet-etch to form the gate, source and drain electrodes of the n and p channels TFTs, as well as the metal interconnects between the two gates, and the two drains of the p TFT and the n TFT. The pull-up p channel TFT and pull-down n channel TFT have 180 μm wide and 45 μm long channels. These

large dimensions result from our use of a laser printer for mask making. The $\beta \equiv (W_p/L_p)/(W_n/L_n)$ of the CMOS inverter, defined as the ratio of the width/length ratio of the pull-up p channel TFT over the width/length ratio of the pull-down n channel TFT, is 1. The TFTs and the inverters were measured with a HP 4155 parameter analyzer using its standard measuring program for FETs and inverters.

3. Results

Fig. 2 shows the transfer characteristics of the p channel TFT of the inverter. In the transfer characteristics the drain current, I_d , vs gate voltage, V_{gs} , was measured for drain voltages, V_{ds} , of -0.1 and -10 V. We define the ON current, I_{ON} , as the drain current, I_d , at a gate voltage, V_{gs} , of -25 V, and the OFF current, I_{OFF} , as the smallest drain current at a drain voltage of V_{ds} of -10 V. Fig. 2 shows a p channel TFT ON/OFF current ratio of $>10^3$ when the gate voltage swings from -10 to -25 V, a threshold voltage, V_{TH} , of -16 V, and a subthreshold slope, $S \equiv dV_{gs}/d \log_{10} I_d$, of 2.7 V/decade. The hole field-effect mobilities, μ_{th} , of the p channel TFT extracted from the linear and saturated regimes are 0.023 and 0.031 $\text{cm}^2/\text{V s}$, respectively.

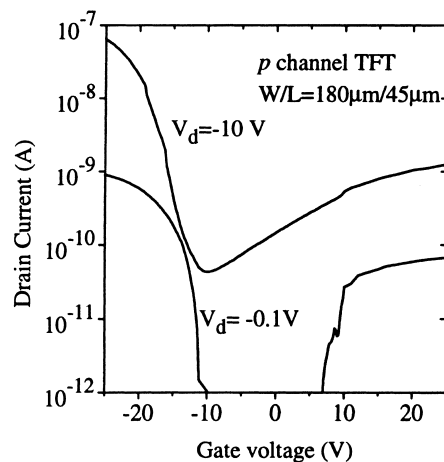


Fig. 2. Transfer characteristics of the p channel $\mu\text{-Si}$ TFT of the CMOS inverter.

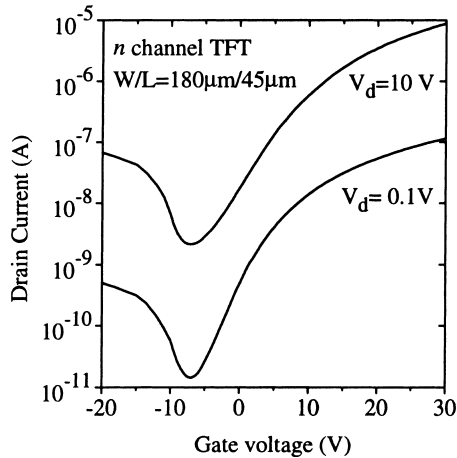


Fig. 3. Transfer characteristics of the *n* channel μ -Si TFT of the CMOS inverter.

Fig. 3 shows the transfer characteristics of the *n* channel TFT of the inverter. The drain current, I_d , vs gate voltage, V_{gs} , was measured for drain voltages, V_{ds} , of 0.1 and 10 V. We define the ON current, I_{ON} , as the drain current, I_d , at a gate voltage, V_{gs} , of 25 V, and the OFF current, I_{OFF} , as the smallest drain current at a drain voltage of V_{ds} , of 10 V. The ON/OFF current ratio of the *n* channel TFT of Fig. 3 is $\sim 10^4$, its V_{TH} is 3 V, and $S = 4.2$ V/decade. The electron field-effect mobilities, μ_n , of the *n* channel TFT extracted from the linear and saturated regimes are 0.72 and 1.0 $\text{cm}^2/\text{V s}$, respectively.

The voltage transfer characteristic of the first μ -Si CMOS inverter made of the pull-up *p* channel TFT and the pull-down *n* channel TFT is shown in Fig. 4 for supply voltages of $V_{DD} = 30$ V and $V_{SS} = -20$ V. The inverter has a nearly full rail-to-rail swing, and a well-defined voltage transfer characteristic with a gain of 7.2, measured from the slope of the voltage transfer curve in the transition region. The output HIGH is about 90% of the full voltage range and the output LOW is at the same voltage as V_{SS} .

4. Discussion

The linear and saturated hole mobilities in the *p* channel TFT are 0.023 and 0.031 $\text{cm}^2/\text{V s}$, re-

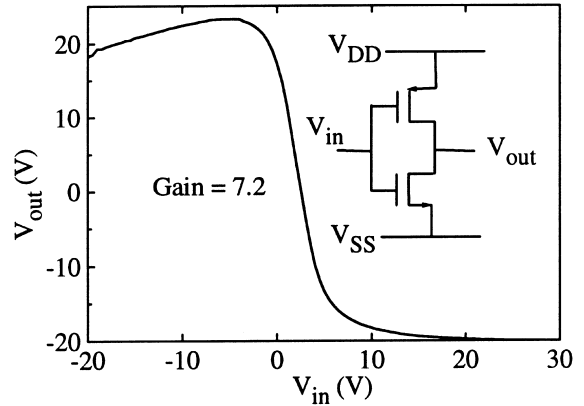


Fig. 4. Voltage transfer characteristics of a CMOS inverter made of μ -Si. The *p* and *n* channels TFTs have identical channel dimensions. $V_{DD} = 30$ V and $V_{SS} = -20$ V.

spectively. While these values are small compared to those of *n* channel TFTs, they do demonstrate *p* channel operation. The threshold voltage of -16 V indicates that the channel film may be slightly *n* type, so that it needs extra gate voltage to invert the conducting channel. For a threshold voltage shift of ~ -10 V of the TFT compared to the TFT with a channel free of *n* type dopant, we deduce an effective interior *n* type dopant density of $\sim 1 \times 10^{17} \text{ cm}^{-3}$, using the following formula [17]:

$$V_{TH} = V_{FB} - 2\phi_p - (4\epsilon_s q N_d \phi_p)^{1/2} / C_{ox}, \quad (1)$$

where V_{FB} is the flat band voltage, ϕ_p the bulk potential, ϵ_s the dielectric constant of silicon, q the electronic charge, N_d the effective *n* type dopant density and C_{ox} is the gate capacitance per unit area.

For the *n* channel TFT the linear and saturated μ_n of 0.72 and 1.0 $\text{cm}^2/\text{V s}$, respectively, are less than those obtained in a separately fabricated μ -Si *n* channel TFT [11]. We ascribe the reduction in field-effect mobility to the unoptimized process sequence for CMOS inverter fabrication, which also is observed in V_{TH} and S . The CMOS inverter has an almost full rail-to-rail output voltage swing and a transition. The output HIGH does not reach V_{DD} because of the smaller ON current of the *p* channel TFT, and the larger leakage current of the *n* channel TFT

at larger negative gate bias. The larger leakage current can be explained by thermionic field emission of carriers through the grain boundary trap states [18].

The $\mu\text{-Si}$ TFTs need improvements in two directions. One is larger field-effect mobilities, to enable larger ON current for greater speed and fan-outs. The other is a further reduction in process temperature, to take advantage of a wider variety of substrate materials. The inverter must be redesigned with a larger β to optimize its performance.

5. Conclusion

We report the first p channel TFT made of directly deposited $\mu\text{-Si}$. The $\mu\text{-Si}$ channel material is grown by PECVD at 320°C and the highest post-deposition TFT process temperature is 280°C . By integrating this p TFT with its n channel counterpart on a single $\mu\text{-Si}$ film, we fabricated the first CMOS inverter of deposited $\mu\text{-Si}$. The low-temperature p channel $\mu\text{-Si}$ TFT and the integrated CMOS inverter represent a digital device and circuit technology based on directly deposited microcrystalline thin film silicon. Its maximum process temperature of 320°C is ideally suited to glass substrates. It also is suited as a CMOS technology for add-on circuits to ASICs.

References

- [1] S. Wagner, H. Gleskova, J.C. Sturm, Z. Suo, Novel processing technology for macroelectronics, in: R.A. Street (Ed.), *Technology and Applications of Hydrogenated Amorphous Silicon*, Springer, New York (to be published).
- [2] B. Schneider, P. Rieve, M. Böhm, in: B. Jähne, H. Haußecker, P. Geißler (Eds.), *Handbook of Computer Vision and Applications*, vol. 1, Academic Press, Boston, MA, 1998, p. 237.
- [3] K. Suzuki, *SID Digest* 167 (1994).
- [4] Y. Okada, J. Chen, I.H. Campbell, P.M. Fauchet, S. Wagner, *Mater. Res. Soc. Symp. Proc.* 149 (1989) 93.
- [5] M. Taguchi, S. Wagner, *Mater. Res. Soc. Symp. Proc.* 358 (1995) 739.
- [6] T. King, *AMLCDs '95 Workshop Proc.* 80, 1995.
- [7] T. Nagahara, K. Fujimoto, N. Kohno, Y. Kashiwagi, H. Kakinoki, *Jpn. J. Appl. Phys.* 31 (1992) 4555.
- [8] J. Woo, H. Lim, J. Jang, *Appl. Phys. Lett.* 65 (1994) 1644.
- [9] H. Meiling, A.M. Brockhoff, J.K. Rath, R.E.I. Schropp, *Mater. Res. Soc. Symp. Proc.* 508 (1998) 31.
- [10] Y. Chen, S. Wagner, *Electrochem. Soc. Proc.* 98-22 (1998) 221.
- [11] Y. Chen, S. Wagner, *Mater. Res. Soc. Symp. Proc.* 557 (1999) (in press).
- [12] J. Jang, S. Koh, T. Kim, S. Kim, *Appl. Phys. Lett.* 60 (1993) 2874.
- [13] Y. Chen, M. Taguchi, S. Wagner, *Mater. Res. Soc. Symp. Proc.* 424 (1997) 103.
- [14] H. Kakinuma, M. Mohri, T. Tsuruoka, *Jpn. J. Appl. Phys.* 77 (1995) 646.
- [15] M. Nakata, PhD thesis, Tokyo Institute of Technology, 1992.
- [16] Y. Okada, PhD thesis, Princeton University, 1990.
- [17] R. Muller, T. Kamins, *Device Electronics for Integrated Circuits*, Wiley, New York, 1986, p. 398.
- [18] S. Bhattacharya, S. Banerjee, B. Nguyen, P. Tobin, *IEEE Trans. Electron Devices* 41 (1994) 221.